Genes, Brain and Behavior
Official publication of the International Behavioural and Neural Genetics Society

Genes, Brain and Behavior (2016) ***15:*** *405–419* doi: 10.1111/gbb.12287

Structure-function integrity of the adult hippocampus depends on the transcription factor Bcl11b/Ctip2

R. Simon[†], L. Baumann[†,‡], J. Fischer[†], F. A. Seigfried[†,§], E. De Bruyckere[†], P. Liu[¶], N. A. Jenkins[**], N. G. Copeland[**], H. Schwegler[††] and S. Britsch[†,*]

[†]Institute of Molecular and Cellular Anatomy, Ulm University, Ulm, [‡]Institute of Pathology and Neuropathology, University of Tübingen, Tübingen, [§]Institute of Biochemistry and Molecular Biology, Ulm University, Ulm, Germany, [¶]Wellcome Trust Sanger Institute, Cambridge, UK, [**]Houston Methodist Research Institute, Houston, TX, USA, and [††]Institute of Anatomy, Otto-von-Guericke-University, Magdeburg, Germany
**Corresponding author: Prof S. Britsch, Institute of Molecular and Cellular Anatomy, Ulm University, Albert-Einstein-Allee 11, 89081 Ulm, Germany. E-mail: stefan.britsch@uni-ulm.de*

The dentate gyrus is one of the only two brain regions where adult neurogenesis occurs. Throughout life, cells of the neuronal stem cell niche undergo proliferation, differentiation and integration into the hippocampal neural circuitry. Ongoing adult neurogenesis is a prerequisite for the maintenance of adult hippocampal functionality. Bcl11b, a zinc finger transcription factor, is expressed by postmitotic granule cells in the developing as well as adult dentate gyrus. We previously showed a critical role of Bcl11b for hippocampal development. Whether Bcl11b is also required for adult hippocampal functions has not been investigated. Using a tetracycline-dependent inducible mouse model under the control of the forebrain-specific *CaMKIIα* promoter, we show here that the adult expression of *Bcl11b* is essential for survival, differentiation and functional integration of adult-born granule cell neurons. In addition, Bcl11b is required for survival of pre-existing mature neurons. Consequently, loss of *Bcl11b* expression selectively in the adult hippocampus results in impaired spatial working memory. Together, our data uncover for the first time a specific role of Bcl11b in adult hippocampal neurogenesis and function.

Keywords: Adult neurogenesis, Bcl11b, dentate gyrus, hippocampus, spatial memory

Received 28 August 2015, revised 22 December 2015 and 16 February 2016, accepted for publication 22 February 2016

Hippocampal structures execute important functions in spatial learning and memory in mice. It requires high plasticity of the neuronal circuitries to acquire and process new as well as retrieve already stored information. Adult neurogenesis contributes to accomplish these tasks by generating new neurons from neuronal stem cells of the subgranular zone (SGZ) of the dentate gyrus, one of the two mammalian brain regions where neurogenesis occurs throughout adulthood (reviewed in Deng *et al.* 2010). The unique processes of dentate gyrus development involving specific molecular pathways allow for adult neurogenesis to occur (Li & Pleasure 2005, 2007). Formation of the dentate gyrus primordium starts early in embryonic development; however, more than 80% of neurons are born within the first 4 weeks of postnatal development establishing the granule cell layer (GCL) consisting of postmitotic neurons (Altman & Bayer 1990; Muramatsu *et al.* 2007). During this process, the progenitor cells are migrating to the SGZ of the dentate gyrus located between GCL and hilus providing the stem cell pool for continuing adult neurogenesis (Altman & Bayer 1990). Neurogenesis was defined initially by proliferation of progenitor cells only, which did not distinguish between progenitor cell renewal and developing neurons. However, developing neurons pass through a series of stages such as migration, differentiation, maturation and integration. Decisions for survival or the direction of further development of each cell has to be taken at each step. Therefore, neurogenesis is nowadays defined as an ongoing process from proliferating progenitor cell to functional integrated mature neuron including all intermediate steps (Kempermann 2011). Neurogenesis during hippocampal development and in adulthood is regulated by similar, overlapping as well as non-overlapping mechanisms. Regulation of adult neurogenesis and maintenance of the adult hippocampus are so far incompletely characterized. Neurons of the developing postnatal dentate gyrus as well as adult-born neurons are both regulated by several factors expressed in a spatio-temporal pattern to ensure a functional hippocampal circuitry (Hsieh 2012; Jiang & Hsieh 2014; Kempermann *et al.* 2004). To activate quiescent stem cells to undergo adult neurogenesis, a whole range of factors, such as Wnt and Notch signaling pathways, are required (Ehret *et al.* 2015; Lie *et al.* 2005; Urban & Guillemot 2014). These signals are regulated by extrinsic factors that can either activate or repress adult neurogenesis. It was shown that stress and aging repress adult neurogenesis (Klempin & Kempermann 2007; Mirescu & Gould 2006) resulting in a decline in learning and memory capacities. Reduced adult neurogenesis is also associated with depression and anxiety, often the first sign of neurodegenerative diseases (Sahay & Hen 2007; Winner & Winkler 2015). In contrast, exercise acts as an extrinsic activating factor by transiently elevating the proliferation of progenitor cells in the SGZ of the dentate gyrus improving learning and memory behavior (Van Praag *et al.* 1999). Moreover, exercise can improve impaired neurogenesis (Farioli-Vecchioli *et al.* 2014) as well as neurogenesis in aged mice (Gibbons *et al.* 2014)

increasing learning and memory capacities. In addition, aging as well as neurodegenerative diseases can cause the degeneration of established mature and integrated neurons leading to behavioral deficits as was shown for epilepsy, Parkinson's and Alzheimer's diseases (Heinrich *et al.* 2006; Pereira *et al.* 2013; Sirerol-Piquer *et al.* 2011).

Previously, we have shown that the zinc finger transcription factor Bcl11b plays an important role in the regulation of neurogenesis during postnatal dentate gyrus development (Simon *et al.* 2012). Ablation of *Bcl11b* expression during development causes reduced progenitor cell proliferation as well as an arrest of neuronal differentiation resulting in a decrease of the dentate gyrus area and cell number. Subsequently, loss of *Bcl11b* expression in the developing hippocampus results in significantly impaired spatial learning and memory (Simon *et al.* 2012).

Bcl11b expression is first observed at embryonic stage 10.5 (E10.5) occurring predominantly in the nasal cavity epithelium and the outer layers of the developing cerebral cortex and at lower levels throughout the embryo (Leid *et al.* 2004). In the prospective hippocampus, *Bcl11b* expression starts in the cornu ammonis (CA) at E15, expands to the suprapyramidal blade of the developing dentate gyrus at E18 and occurs in the maturing granule cells and the CA1 and CA2 regions during perinatal development (Simon *et al.* 2012). In addition to the hippocampus, Bcl11b expression occurs in the neocortex and the striatum regulating prenatal development of corticospinal motor neurons as well as specific subsets of striatal neurons (Arlotta *et al.* 2005, 2008; Chen *et al.* 2008). Bcl11b acts as a transcriptional regulator either sequence-dependent or through co-factors involved in the lymphopoietic system as well as the brain (Avram *et al.* 2000; Cismasiu *et al.* 2006, 2009; Topark-Ngarm *et al.* 2006).

Hippocampal expression of *Bcl11b* is sustained throughout life. However, functions of Bcl11b specific to the adult hippocampus have not been characterized yet. Here, we show that Bcl11b executes crucial functions in adult hippocampal neurogenesis and survival of mature neurons. Conditional forebrain-specific *Bcl11b* mutants exhibit an increasingly severe phenotype at the age of 6 months when compared with the developmental stages. We show that the progressive phenotype is caused by an ongoing depletion of progenitor cell proliferation and arrested granule cell differentiation. To determine whether Bcl11b executes functions specific to adult neurogenesis, we employed the tet-off system under the control of the forebrain-specific *CaMKIIα* promoter (Mayford *et al.* 1996) allowing the induction of the Bcl11b mutation selectively in adulthood. Selective ablation of Bcl11b in the adult dentate gyrus caused an increase in apoptosis and arrest of neuronal differentiation. In turn, this results in a decrease of granule cell numbers and organ size already at 2 months after the loss of Bcl11b. In addition, adult-induced *Bcl11b* mutants display a reduced number of thorny excrescences of the CA3, which might contribute to the observed impairment of spatial learning and memory. Taken together, our data show that Bcl11b is required in adult neurogenesis by regulating the differentiation of adult-born neurons as well as the survival of mature neurons. Ablation of Bcl11b in adulthood results in early morphological changes leading to functional impairment.

Material and methods

Animals

Generation of *Bcl11b*$^{flox/flox}$ is described elsewhere (Li *et al.* 2010). *Bcl11b*$^{flox/flox}$ mice were cross-bred either with the forebrain-specific *Emx1-Cre* (Gorski *et al.* 2002; conditional system) or with *tetO-Cre* and *CaMKIIα-tTA* (Mayford *et al.* 1996; inducible system) mouse lines. Expression of *Emx1-Cre* occurs in mitotic as well as in postmitotic cells as early as E10.5 (Gorski *et al.* 2002; Simon *et al.* 2012). *CaMKIIα* is expressed predominantly in adulthood and restricted to postmitotic cells of the forebrain (Burgin *et al.* 1990; Mayford *et al.* 1996). *Bcl11b*$^{flox/flox}$; *tetO-Cre* mice were cross-bred with *Bcl11b*$^{flox/flox}$; *CaMKIIα-tTA* mice to generate *Bcl11b*$^{flox/flox}$; *tetO-Cre* (control) and *Bcl11b*$^{flox/flox}$; *CaMKIIα-tTA*; *tetO-Cre* (mutant) mice. The conditional *Bcl11b*$^{flox/flox}$; *Emx1-Cre* mice have a mixed C57BL/6xSv/129 and mice used in the inducible system have a mixed C57BL/6xSv/129xNMRI genetic background. Animals used in the experiments were taken from the F2 generation onwards. All animals were group-housed except for the duration of the behavioral studies. For behavioral studies, animals were single-housed 1 week before the start of the experiments. Behavioral tests were conducted during the light phase, consecutively one test per day without an inter-test interval. The same animals were used in all behavioral tests. Mice of the inducible system were administered doxycycline (50 mg/l; Sigma-Aldrich, cat. #: D9891; St Louis, Missouri, USA) with the drinking water throughout embryogenesis up to 2 months of age. Experiments were performed at 2 and 4 months after doxycycline removal. Genotyping of the mice was performed by polymerase chain reaction (PCR). All animal experiments were carried out in accordance with the German law and were approved by the government offices in Tübingen, Germany.

Histology, immunohistology, Timm and Golgi impregnation

Morphological analysis was performed on 5-μm methacrylate sections (Technovit 7100, Heraeus-Kulzer, Wehrheim, Germany) using 0.02% cresyl violet/0.2 M Walpole buffer (Chroma-Waldeck, Münster, Germany) for 30 min at room temperature.

For immunofluorescence staining, brain tissues were fixed with 4% paraformaldehyde in 0.1 M sodium phosphate buffer (pH 7.4). Cryosections of 12–14 μm were obtained from matched control and mutant brains. The sections were treated with the following antibodies: goat anti-NeuroD and mouse anti-NeuN (all Santa Cruz, Dallas, TX, USA), rabbit anti-Calbindin (Swant, Marly, Switzerland), rabbit anti-Sox2 (Millipore, Billerica, MA, USA), rat anti-BrdU (AbD Serotec, Puchheim, Germany) and rabbit anti-Tbr2 (Abcam, Cambridge, UK). Generation of an anti-Bcl11b antibody was described elsewhere (Simon *et al.* 2012). Stained sections were examined on a confocal microscope (Leica Sp5II, Wetzlar, Germany).

For the Timm staining, mice were transcardially perfused with buffered sodium sulfate and glutaraldehyde, placed overnight in a 30% saccharose solution followed by embedding in Polyfreeze Tissue Freezing Medium (Polysciences, Inc. Warrington, PA, USA; cat. #: 19636). Cryosections of 40 μm were developed in Timm's solution as was described in Schwegler and Lipp (1983).

Golgi staining of hippocampal tissue was carried out according to a modified protocol published previously (Heimrich & Frotscher 1991).

Determination of progenitor cell proliferation and apoptosis

Progenitor cell proliferation was determined by BrdU incorporation. Adult animals at the appropriate age were injected intraperitoneally with BrdU (100 μg/g body weight; Sigma-Aldrich, St. Louis, MO, USA cat. #: B9285) on three successive days at the same time of day according to established protocols (Kempermann *et al.* 2003; Mathews *et al.* 2010). Brains were dissected either on day 4 or day 28 after the first injection to determine the proliferation, survival and differentiation rate of adult-born neurons. Apoptotic cells were detected by TUNEL assay according to the manufacturer's manual (Millipore, Billerica, MA, USA cat. #: S7110).

Determination of cell numbers and area

Forebrain tissues of at least three mutant and control animals were sectioned serially (5 μm sections) followed by cresyl-violet staining. Dentate gyrus cell number and area were determined on three (conditional system) or nine (inducible system) matched sections of the caudal, medial as well as the rostral hippocampus per animal using ImageJ 1.48V and the average value of a section per animal was determined. The cell number of the CA1 region was determined by counting cells of a fixed sized rectangle of nine matched sections of the caudal, medial and rostral hippocampus per animal.

Determination of dendritic spines, thorny excrescences as well as mossy fiber areas

Three Golgi-impregnated control and *Bcl11b* mutant hippocampi sections of 100 μm were used to determine the dendritic spine number of the dorsal and ventral dentate gyrus granule cells as well as the thorny excrescences located in the apical dendritic tree of CA3 pyramidal neurons. To determine the dendritic spine number, selected dendrites were divided into 50 μm sections starting from the cell soma to the end of the dendrites. At least 15 neurons and a total of 7000 spines per animal were counted. Thorny excrescences were identified according to the previously published morphological criteria (Gonzales *et al.* 2001) and counted within the first 50 μm from the soma of the apical dendrites of CA3 pyramidal cells corresponding to the stratum lucidum. At least 7–10 neurons per animal and 200 thorny spines per neuron were counted.

Real-time RT-PCR

Quantitative reverse transcriptase (qRT)-PCR assays were described elsewhere (Simon *et al.* 2012). Briefly, total RNA of four control and mutant hippocampi was isolated using RNeasy Minikit (Qiagen, Hilden, Germany) and reverse transcribed with Superscript™II Reverse Transcriptase (Invitrogen, Carlsbad, CA, USA). Quantitative real-time RT-PCR was performed using the Light Cycler®480 SYBR Green I Master kit (Roche, Basel, Switzerland cat. #: 04707516001) in a Light Cycler 480 System (Roche, Basel, Switzerland). The following specific primers were used: Bcl11b: 5′-TGGATGCCAGTGTGAG TTGT-3′ and 5′-AATTCATGAGTGGGGACTGC-3′; Desmoplakin (Dsp): 5′-CGGACATTCATGCGAGATAC-3′ and 5′-GCCTTGAACTGGGAACA CTC-3′ as well as GAPDH as internal control: 5′-CCAGAGCTGAACGG GAAG-3′ and 5′-TGCTGTTGAAGTCGCAGG-3′. The relative copy number of GAPDH RNA was quantified and used for normalization. Data were analyzed using the $2^{-\Delta\Delta C_T}$ method (Livak & Schmittgen 2001).

Behavioral tests

Behavioral analyses were performed employing adult male wild-type and mutant animals in the open field (horizontal and vertical activity), elevated plus maze (anxiety-related behavior) and a spatial version of a radial arm maze. Control and mutants were age matched and of the same genetic background (C57BL/6xSv/291xNMRI). Open field, elevated plus maze as well as radial arm maze tests are described elsewhere (Schwegler *et al.* 1990; Yilmazer-Hanke *et al.* 2004). Briefly, the open field test was performed in a box divided up by squares and placing the mice on the central square. Locomotor activity (number of line crossings), rearings (standing upright on the hindlegs) and leanings (standing on the hindlegs and touching the wall with the forelegs) were recorded during a 10-min session (Yilmazer-Hanke *et al.* 2004). The distance traveled was estimated by multiplying the number of line crossings with the factor 10 (squares of 10 cm). The elevated plus maze consisted of a wooden apparatus, elevated 83 cm above the floor with four arms of 30 × 5 cm at right angles connected by a central platform (5 × 5 cm). Two opposing arms were enclosed by a 30-cm high wall (closed arms) and two arms had no walls (open arms). Mice were placed on the central platform, facing a closed arm and were allowed to move freely for 10 min. The absolute and relative numbers of entries in the open and closed arms as well as the absolute and relative cumulative time spent in either arm were measured (Yilmazer-Hanke *et al.* 2004). The radial arm maze consisted of a central octogonial platform with eight regularly arranged Plexiglas arms (25 × 6 × 6 cm) with a hidden food pellet (10 mg) at the end of each arm. Extra-maze cues were placed around the maze. Mice were food-deprived to 85–90% of pre-test body weight. Testing started with two habituation trials (15 min) on two consecutive days with free access to all arms to familiarize the mice with the maze. Starting the following day, a training period of five consecutive days with one trial each day was performed. These were terminated after 15 min (first day) and 10 min on the following 4 days or after all eight rewards were eaten, whatever came first. Repeated entries into one arm, time spent in the maze till all rewards had been eaten and the numbers of novel entries within the first eight entries were counted and scored (Schwegler *et al.* 1990).

Statistical analysis

Results are expressed as the mean ± SEM or mean ± SD (quantitative real-time RT-PCR). Comparisons between groups were made by an unpaired one-tailed Student's *t*-test due to the hypothesis based on previous data (Simon *et al.* 2012) using the SPSS version 21 program. We expect that the examined parameters, e.g. dentate gyrus area, number of granule cells, apoptosis, differentiation and behavior, of the adult animals are progressing in the same direction as found for postnatal development. Quantitative RT-PCR data were analyzed using the $2^{-\Delta\Delta C_T}$ method as described previously (Livak & Schmittgen 2001). A two-way analysis of variance with dependent variables was performed for the analysis of the radial arm maze data. Differences in value were considered to be significant at $P < 0.05$.

Results

Bcl11b expression is required in adult neurogenesis

Bcl11b is first expressed in the CA region at E15 and expands to the suprapyramidal band of the developing dentate gyrus at E18. As early as postnatal stage P7, *Bcl11b* expression occurs in postmitotic granule cells of the dentate gyrus and cells of the CA1 and CA2 region and is sustained throughout adulthood (Fig. 1a; Simon *et al.* 2012). To determine whether Bcl11b is required during adult neurogenesis, after postnatal development is concluded, we examined the hippocampus of 6-month-old control and *Bcl11b*$^{flox/flox}$; *Emx1-Cre* (conditional mutant) animals. We found a reduction of the dentate gyrus area by 50% (control = 100 ± 6.8%, mutant = 49.6 ± 1.6%; $P = 0.001$) and number of granule cells by 45% (control = 1326 ± 99, mutant = 731 ± 51; $P = 0.003$) of *Bcl11b* mutants when compared with control animals (Fig. 1c–j). A more dramatic reduction of the granule cell number as well as the area was detected in the infrapyramidal blade (cell number: control = 607 ± 23, mutant = 226 ± 13, $P = 0.0002$; area: control = 38.7 ± 2.5%, mutant = 14.1 ± 1.0%, $P = 0.0002$; Fig. 1g–j) in comparison to the suprapyramidal blade (cell number: control = 719 ± 76, mutant = 505 ± 38, $P = 0.039$; area: control = 61.3 ± 4.3%, mutant = 36.4 ± 1.5%, $P = 0.003$; Fig. 1e,f,i,j). Comparing the dentate gyrus area and granule cell numbers of 6-month-old and P30 (Simon *et al.* 2012) animals showed an additional 10% reduction of the dentate gyrus area and 12% decrease in the number of granule cells of 6-month-old animals.

The further reduction of size and cell number of the dentate gyrus could be due to either impaired survival of neurons and/or a decrease in progenitor cell proliferation. To determine the number of proliferating cells, 6-month-old animals were injected with BrdU on three successive days followed by brain dissection either on day 4 or day 28 after

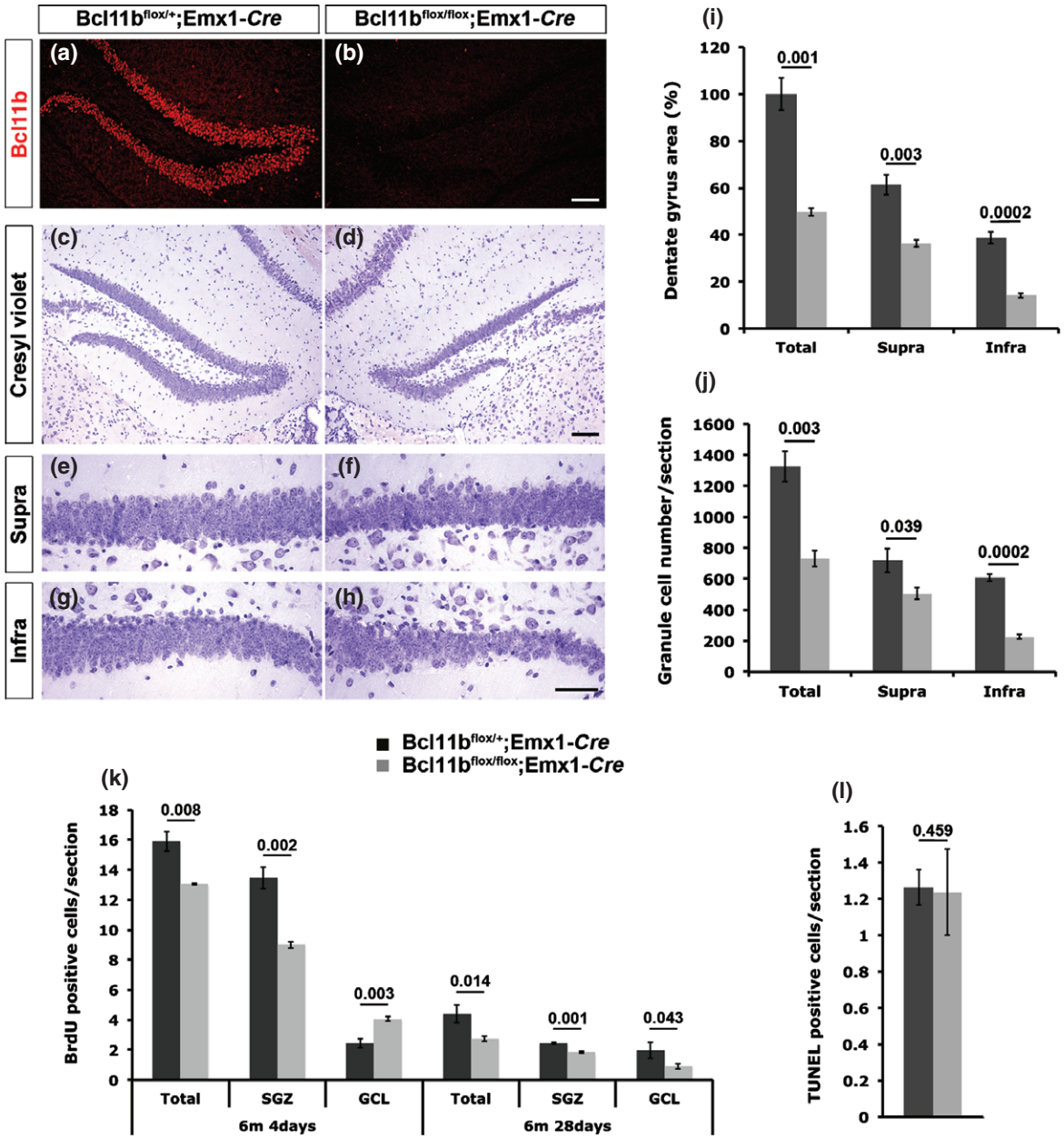

Figure 1: Conditional *Bcl11b* mutants exhibit a progressive phenotype at 6 months of age. (a,b) Immunofluorescence staining of 6-month-old hippocampal control (a) and conditional *Bcl11b* mutant (b) sections. (c–h) Cresyl violet staining of plastic sections of control (c,e,g) and conditional *Bcl11b* mutant (d,f,h) hippocampi. (i,j) Quantitative analysis of the dentate gyrus area (i) and granule cell number (j). (k,l) Quantitative analysis and distribution of BrdU at 4 (4d) and 28 (28d) days after the initial BrdU injection (k) and TUNEL (l), positive cells of control and conditional *Bcl11b* mutant hippocampi sections. Supra, suprapyramidal blade; Infra, infrapyramidal blade; scale bar, 25 μm (h), 75 μm (b) and 100 μm (d); *t*-test, numbers indicate *P*-values; error bars, SEM; $n = 3$ (k; 4 days mutant; 28 days control; l), $n = 4$ (i–j; k: 4 days control; 28 days mutant).

the initial injection. The BrdU-positive cells were reduced by 18.2% at day 4 (control = 15.9 ± 0.7, mutant = 13.0 ± 0.1; $P = 0.008$; Fig. 1k) and 37.5% at day 28 (control = 4.4 ± 0.5, mutant = 2.75 ± 0.2; $P = 0.014$; Fig. 1k) in mutants when compared with controls most likely causing the progressive reduction of the dentate gyrus area and cell number. No difference was found in the number of apoptotic cells of 6-month-old control and conditional *Bcl11b* mutant animals as assessed by TUNEL assays (control = 1.3 ± 0.1, mutant = 1.2 ± 0.2; $P = 0.459$; Fig. 1l). At day 4 after the

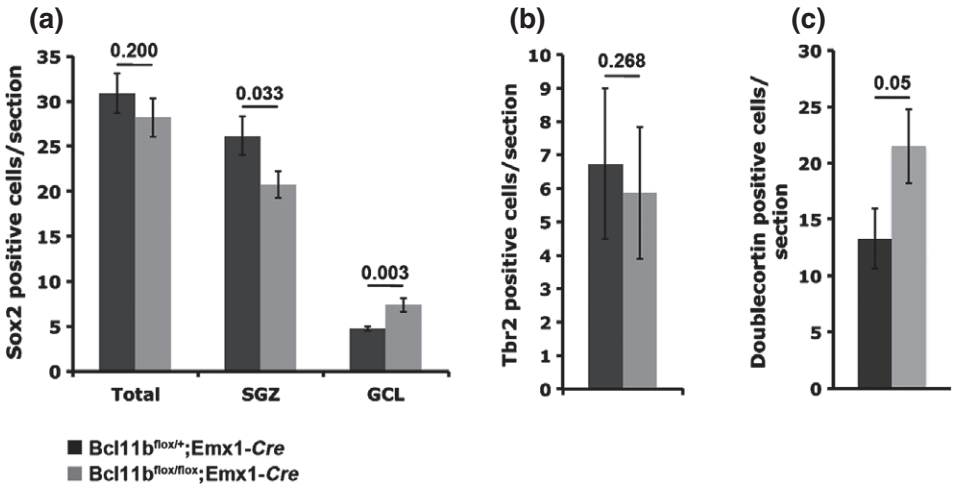

Figure 2: ***Bcl11b*** **expression is required for the differentiation of adult-born neurons.** Quantitative analysis and distribution of genes involved in adult neurogenesis, *Sox2* (a), *Tbr2* (b) and *Doublecortin* (c). *t*-test, numbers indicate *P*-values; error bars, SEM; $n = 6$ (a), $n = 5$ (b); $n = 3$ (c).

first injection, BrdU-positive cells were misdistributed with fewer BrdU-positive cells in the SGZ (control = 13.5 ± 0.7, mutant = 9 ± 0.2; $P = 0.002$) and more BrdU-positive cells in the GCL (control = 2.4 ± 0.3, mutant = 4.1 ± 0.1; $P = 0.003$) of mutants compared with controls (Fig. 1k). At day 28, a proportional reduction of BrdU-positive cells was observed in both SGZ and GCL of *Bcl11b* mutants compared with controls (SGZ, control = 2.4 ± 0.1, mutant = 1.8 ± 0.1, $P = 0.001$; GCL, control = 2 ± 0.1, mutant = 1.9 ± 0.1, $P = 0.043$; Fig. 1k).

To further elucidate the functions of Bcl11b in progenitor cell proliferation during adult neurogenesis, we analyzed the expression of *Sox2* and *Tbr2*, identifying type 1/2a and 2b/3 progenitors, respectively. While the overall numbers of *Sox2* (control = 30.9 ± 2.3, mutant = 28.2 ± 2.1; $P = 0.200$; Fig. 2a) and *Tbr2* (control = 6.7 ± 0.9, mutant = 5.8 ± 0.8; $P = 0.268$; Fig. 2b) positive cells were unchanged, *Sox2*-expressing cells were significantly increased in the GCL (control = 4.7 ± 0.2, mutant = 7.4 ± 0.7; $P = 0.003$) at the expense of cells in the SGZ (control = 26.2 ± 2.1, mutant = 20.8 ± 1.5; $P = 0.033$; Fig. 2a). Furthermore, numbers of cells expressing *Doublecortin*, which identifies late mitotic and early postmitotic differentiation stages, were significantly increased in mutants compared with controls (control = 13.3 ± 2.7, mutant = 21.5 ± 3.3; $P = 0.049$; Fig. 2c). Together, this suggests that in *Bcl11b* mutants progenitor cells, as identified by the expression of *Sox2*, are no longer confined to their stage-specific environment and Bcl11b is required for granule cell differentiation.

Bcl11b is required for the differentiation of adult-born neurons

To directly assess the differentiation capacity of adult-born granule cells, we analyzed the expression of marker genes identifying distinct steps of adult neurogenesis specifically in BrdU-labeled cells of the dentate gyrus (Hsieh 2012; Kempermann *et al.* 2004; Fig. 3e and Table 1): Analyzing the co-localization of either BrdU, Tbr2 and NeuroD (combination 1) or of BrdU, NeuN and Calbindin (combination 2) 4 days after initial BrdU injection, when the majority of BrdU-positive cells still undergo early differentiation, showed a dramatic decrease in immature (BrdU+, Tbr2− and NeuroD+; $P = 0.004$) as well as mature granule cell neurons (BrdU+, NeuN+ and Calbindin+; $P = 0.0002$; Table 1 and Fig. 3a–d) in *Bcl11b* mutants compared with controls. At the same time point, type 2b/3 progenitor cells were increased almost twofold in Bcl11b mutants compared with controls (BrdU+, Tbr2+ and NeuroD+; $P = 0.012$). After 28 days of the initial BrdU injection when the majority of BrdU-labeled cells should have entered late neuronal differentiation, numbers of mature granule cell neurons (BrdU+, NeuN+ and Calbindin+; $P = 0.0002$) as well as type 2a progenitors (BrdU+, Tbr2+ and NeuroD−; $P = 0.050$) were found severely reduced (Table 1 and Fig. 3b,d) in mutants compared with controls. In contrast, type 2b/3 (BrdU+, Tbr2+ and NeuroD+; $P = 0.033$) and immature cells (BrdU+, Tbr2− and NeuroD+; $P = 0.001$ and BrdU+, NeuN+ and Calbindin−; $P = 0.007$) were dramatically increased in mutants compared with controls (Table 1 and Fig. 3a–d). At both time points, we noticed that cells solely expressing BrdU were significantly reduced in mutants (BrdU+, Tbr2− and NeuroD−; $P = 0.019$ at 4 days, $P = 0.012$ at 28 days after the initial BrdU injection). Depending on the time point of analysis, the majority of BrdU only cells most likely correspond to different types of cells, either type 1 progenitors (4 days) or mature neurons (28 days; Table 1 and Fig. 3a–d). Taken together, these data suggest that neuronal differentiation of adult-born granule cells depends on Bcl11b. Over time, this results in the arrest of most of the mutant cells at the level of transition from type 2b/3 progenitors to immature postmitotic neurons. Thus, only few adult-born *Bcl11b* mutant neurons reach maturity.

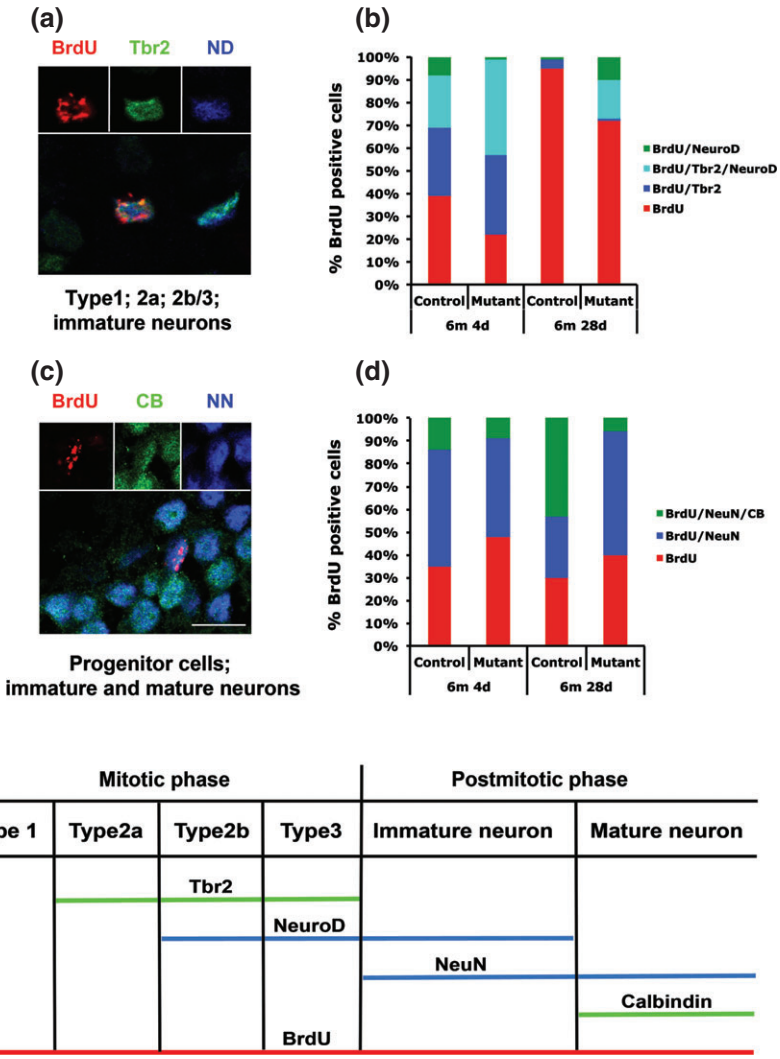

Figure 3: Differentiation analysis of adult-born granule cells. (a,c) Immunofluorescence staining of BrdU (red), Tbr2 (green) and NeuroD (blue) (a) as well as BrdU (red), CB (green) and NeuN (blue) (c) positive cells. Scale bar, 7.5 μm. (b,d) Schematic representation of the quantitative analysis of co-localization of BrdU, Tbr2 and NeuroD (b) as well as BrdU, Calbindin and NeuN (d). $n=3$; NN, NeuN; ND, NeuroD; CB, Calbindin. (e) Alignment of marker genes used to their respective differentiation stages.

Adult-induced Bcl11b ablation using the tet-off system

Analysis of the aging *Bcl11b*$^{flox/flox}$; *Emx1-Cre* mice indicate a progressive phenotype but it remains to be determined whether this is because of the loss of *Bcl11b* expression during development or an isolated role of Bcl11b during adult neurogenesis. To answer this, we introduced the tet-off system into the *Bcl11b*$^{flox/flox}$ mouse line. *Dsp* to prevent the induction of the *Bcl11b* mutation prematurely, doxycycline was administered during embryogenesis and postnatal development up to 2 months of age (Fig. 4a). To determine the efficiency of the tet-off system (Mayford *et al.* 1996), we examined the mRNA expression levels of *Bcl11b* and its direct downstream target gene, (Simon *et al.* 2012), in the hippocampus of 3-month-old mice either administered doxycycline at all times (+Dox) or up to the age of 2 months (−Dox). While there is no significant difference in the mRNA expression levels of *Bcl11b* and *Dsp* in animals administered doxycycline at all times, the expression levels are dramatically reduced in animals where doxycycline was withheld in adulthood (Bcl11b reduction: 94% ± 0.6/0.6; $P=0.0004$; Dsp reduction: 78.6% ± 3.8/4.6; $P=0.004$; Fig. 4b). Accordingly, Bcl11b protein was detected in the dentate gyrus of control as well as mutant animals receiving doxycycline at all times but was absent in the hippocampus of *Bcl11b* mutants after 4 weeks of doxycycline removal (Fig. 4c).

Bcl11b expression is required for granule cell survival

The morphology of the dentate gyrus at 2 (2m-Dox) and 4 (4m-Dox) months after the removal of doxycycline showed a significant reduction of the dentate gyrus area as well as reduced granule cell number (Fig. 5a–f). At 2m-Dox, we observed a reduction of the dentate gyrus area by 33% ($P=0.001$; Fig. 5i) and the granule cell number by 28.7% (control = 896.6 ± 36.3, mutant = 639.5 ± 41.8; $P=0.001$; Fig. 5j) when compared with controls. Furthermore, we observed a changed morphology of surviving mutant granule cells. These cells appeared to be smaller, more condensed in comparison to control cells possibly indicating initial stages of degeneration and premature cell death (Fig. 5c–f).

Table 1: Analysis of the differentiation of adult-born granule cells. Quantitative analysis of co-localization of BrdU, Tbr2 and NeuroD (marker combination 1) as well as BrdU, Calbindin and NeuN (marker combination 2) at 4 and 28 days after the initial BrdU injection. Combination 1: Type 1 (4 days after the initial injection) and mature neurons (28 days after the initial injection) (BrdU only); Type 2a (BrdU/Tbr2); Type 2b/3 (BrdU/Tbr2/NeuroD); immature neurons (BrdU/NeuroD). Combination 2: progenitor cells (BrdU only); immature neurons (BrdU and NeuN); mature neurons (BrdU, NeuN and Calbindin).

			4 days after initial BrdU injection		
Marker expression	Corresponding stages		Control (%)	Mutant (%)	*P*
BrdU+/Tbr2−/NeuroD−	Type 1/(mature neurons)	↓	39.02 ± 0.32	22.3 ± 5.43	**0.019**
BrdU+/Tbr2+/NeuroD−	Type 2a	n.c.	30.15 ± 2.66	34.61 ± 7.26	0.297
BrdU+/Tbr2+/NeuroD+	Type 2b/3	↑	22.89 ± 2.33	42.33 ± 4.97	**0.012**
BrdU+/Tbr2−/NeuroD+	Immature neurons	↓	7.94 ± 1.2	0.76 ± 0.76	**0.004**
BrdU+/NeuN−/Calbindin−	Progenitor cells	n.c.	34.55 ± 4.44	47.69 ± 8.7	0.125
BrdU+/NeuN+/Calbindin−	Immature neurons	n.c.	50.79 ± 2.91	43.34 ± 7.19	0.196
BrdU+/NeuN+/Calbindin+	Mature neurons	↓	14.67 ± 1.53	8.97 ± 2.09	**0.046**
			28 days after initial BrdU injection		
Marker expression	Corresponding stages		Control (%)	Mutant (%)	*P*
BrdU+/Tbr2−/NeuroD−	(Type 1)/mature neurons	↓	94.44 ± 1.11	72.22 ± 6.19	**0.012**
BrdU+/Tbr2+/NeuroD−	Type 2a	↓	4.44 ± 1.11	1.11 ± 1.11	**0.050**
BrdU+/Tbr2+/NeuroD+	Type 2b/3	↑	0 ± 0	16.67 ± 6.67	**0.033**
BrdU+/Tbr2−/NeuroD+	Immature neurons	↑	1.11 ± 1.11	10 ± 0	**0.001**
BrdU+/NeuN−/Calbindin−	Progenitor cells	n.c	30 ± 5.77	40 ± 1.92	0.088
BrdU+/NeuN+/Calbindin−	Immature neurons	↑	26.67 ± 6.67	54.44 ± 1.11	**0.007**
BrdU+/NeuN+/Calbindin+	Mature neurons	↓	43.33 ± 3.33	5.56 ± 1.11	**0.0002**

Data are expressed in % of total number of BrdU-positive cells counted; arrows indicate increase or decrease of parameters determined. *P*, P-value; error bars, SEM; significance, $P \leq 0.05$; $n = 3$. n.c., not changed.

Examining control and *Bcl11b* mutant animals at 4m-Dox showed a reduction of the dentate gyrus area by 20% ($P = 0.01$; Fig. 5i) as well as a reduced cell number of 23.3% (control = 830.8 ± 43.7, mutant = 637.2 ± 19.2; $P = 0.003$; Fig. 5j). We observed a drastic size reduction in the mutant already after the first 2 months following doxycycline removal, but no further significant reduction in the dentate gyrus area or cell number during the following 2 months (Fig. 5i,j). Analyzing the CA1 region of the hippocampus, where *Bcl11b* is also expressed did not show a significant change of the cell number in the induced Bcl11b mutant (control = 104.11 ± 6.5, mutant = 99.59 ± 4.9; $P = 0.606$; Fig. 5g–h,k). To explore the cause of the dentate gyrus size reduction, we examined the number of proliferating progenitor cells as well as apoptotic cells of control and adult-induced *Bcl11b* mutant dentate gyrus. Adult-born neurons were labeled by BrdU incorporation as described above at 2 and 4 months after doxycycline removal and brains were dissected either at day 4 or day 28 after the initial injection. In contrast to the adult conditional phenotype, we did not detect a significant change in the proliferation rate of progenitor cells at day 4 after the initial injections at both time points (2m-Dox: control = 5.5 ± 0.6, mutant = 4.5 ± 0.6, $P = 0.122$; 4m-Dox: control = 5.2 ± 0.9, mutant = 6.0 ± 0.2, $P = 0.229$; Fig. 5l). At day 28 after the initial injection, we found a significant decrease of the survival rate of adult-born neurons at 4 months but not at 2 months after doxycycline removal (2m-Dox: control = 2.4 ± 0.2, mutant = 1.8 ± 0.3, $P = 0.098$; 4m-Dox: control = 2.5 ± 0.3, mutant = 1.6 ± 0.3, $P = 0.039$; Fig. 5l). Examining cell death at these time points on the other hand exhibited an increase of apoptotic cells in the adult-induced mutant by the factors 2.1 and 2.5, respectively (2m-Dox: control = 1.0 ± 0.1, mutant = 2.0 ± 0.3, $P = 0.001$; 4m-Dox: control = 0.2 ± 0.04, mutant = 0.6 ± 0.1, $P = 0.005$; Fig. 5m). While we did not observe a difference in the number of adult-born neurons between controls and mutants at both time points (Fig. 5l; 4 days), there are fewer control and mutant TUNEL-positive cells at 4m-Dox (Fig. 5m) which might explain the stagnation of the size reduction of the dentate gyrus at the later time point. Furthermore, the higher apoptotic rate observed in the induced *Bcl11b* mutant might be the indirect cause of the significant reduction of BrdU-positive cells at 28 days after the initial injection at 4m-Dox (Fig. 5l). Together, these data strongly suggest the requirement of Bcl11b expression for the survival of granule cells of the adult hippocampus.

Adult-induced ablation of Bcl11b causes arrest of granule cell differentiation

We next analyzed the differentiation of adult-born granule cells. Control and adult-induced *Bcl11b* mutant hippocampi were examined at 2 and 4 months after the removal of doxycycline by immunohistochemistry using NeuroD and Doublecortin as markers for late mitotic and early postmitotic granule cells, respectively. We found a significant increase of NeuroD-positive cells by the factors 2.2 and 1.7 in the mutant dentate gyrus at 2 and 4 months after doxycycline removal, respectively (2m-Dox: control = 13.3 ± 2.4, mutant = 29.9 ± 2.6, $P = 0.002$; 4m-Dox:

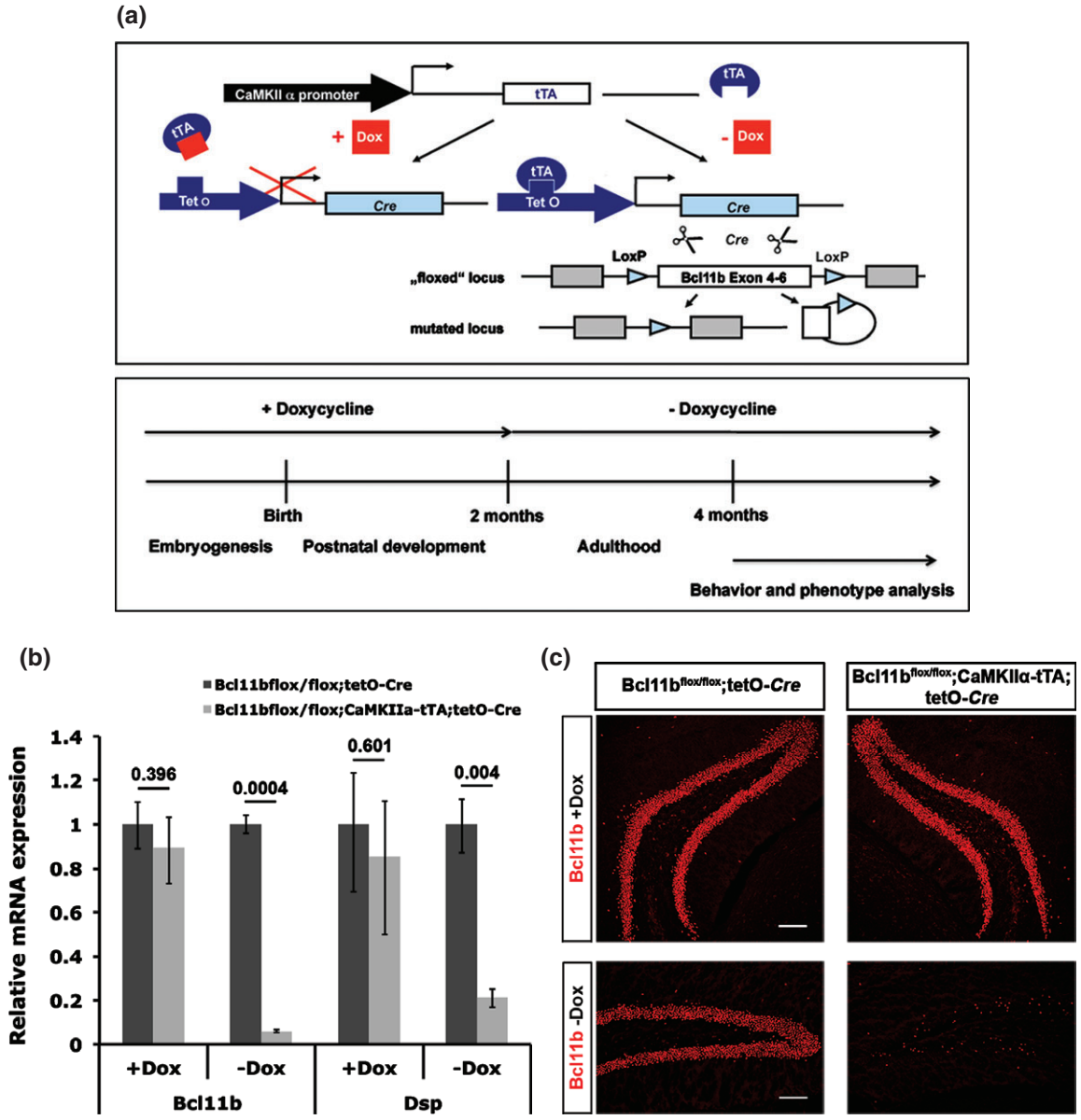

Figure 4: Generation and examination of the adult-induced *Bcl11b* mutation. (a) Schematic representation of the tet-off system and time course of induction of the *Bcl11b* mutation. (b) Quantitative analysis of *Bcl11b* and *Dsp* mRNA expression levels of control and adult-induced *Bcl11b* mutants at 3 months of age administered doxycycline at all times (+Dox) or at 4 weeks after doxycycline removal (−Dox). *t*-test, numbers indicate *P*-values; error bars, SD; $n = 3$. (c) Immunofluorescence staining employing a Bcl11b specific antibody on hippocampal sections of control and *Bcl11b* mutants administered doxycycline at all times (Bcl11b + Dox) and at 4 weeks after doxycycline removal (Bcl11b – Dox). Scale bar, 100 μm.

control = 9.8 ± 0.4, mutant = 16.1 ± 1.3, $P = 0.005$; Fig. 5n). Similarly, Doublecortin-positive cells were increased in induced mutants 4 months without doxycycline (control = 4.20 ± 0.4, mutant = 12.48 ± 3.8; $P = 0.022$; Fig. 5o). Thus, selective ablation of Bcl11b in the adult dentate gyrus results in impaired differentiation of granule cell neurons similar to the phenotype observed in conditional mutant animals.

Loss of Bcl11b expression in adulthood impairs mossy fiber connectivity

To examine whether adult expression of Bcl11b is required for the stability of the mossy fiber tract, we labeled mossy fiber terminals of *Bcl11b* mutant and control hippocampi harvested 2 and 4 months after doxycycline removal by Timm staining. While we did not observe a marked change in the overall mossy fiber distribution (Fig. 6a,b),

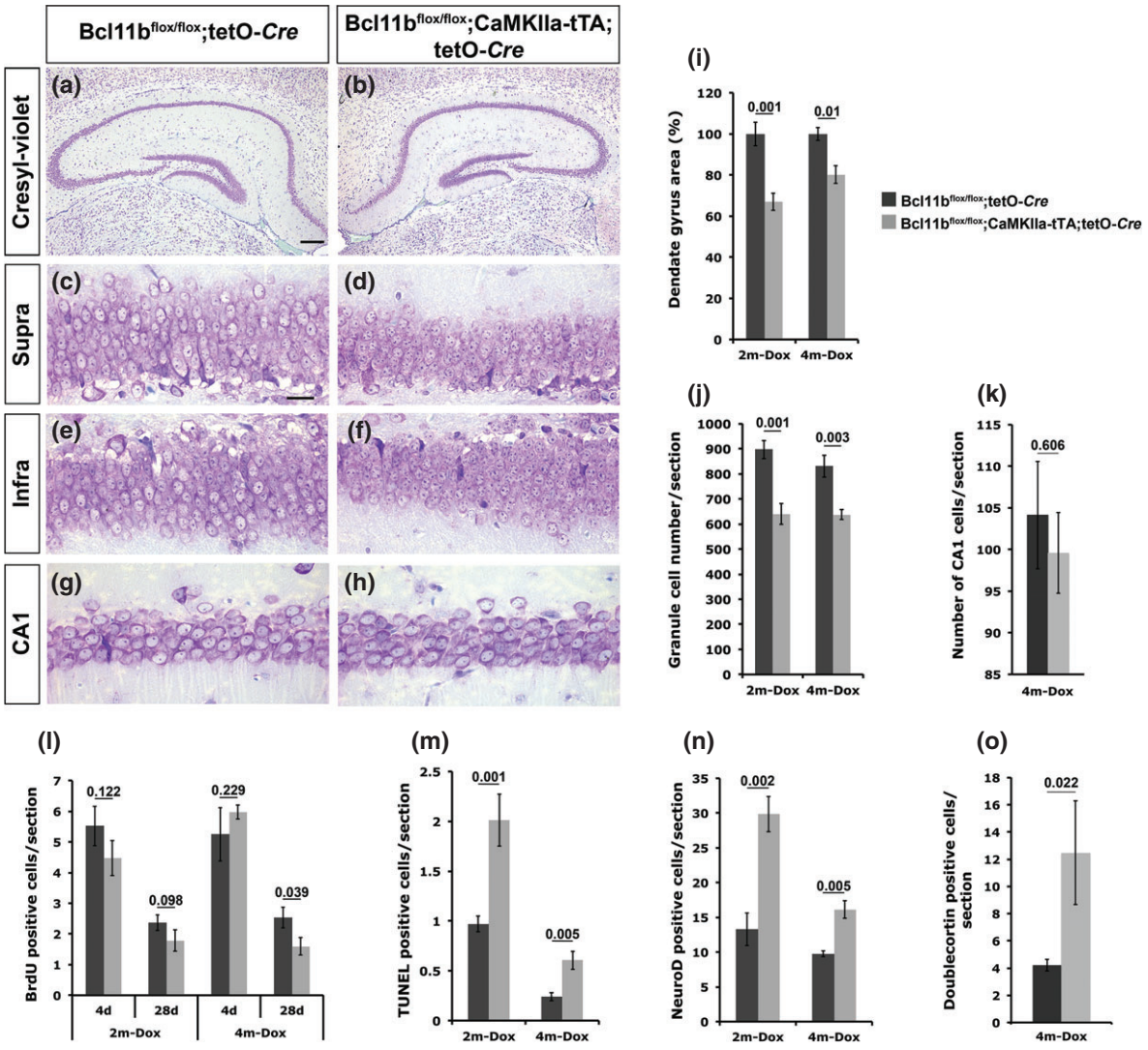

Figure 5: Analysis of adult-induced *Bcl11b* mutant mice at 2 and 4 months after doxycycline removal. (a–h) Cresyl-violet staining of control (a,c,e,g) and *Bcl11b* mutant (b,d,f,h) hippocampal sections at 2 months after doxycycline removal. Scale bar, 20 μm (c); 100 μm (a). (i-o) Quantitative analysis of the dentate gyrus area (i), granule cell number (j), CA1 cell number (k), BrdU incorporation at 4 (4d) and 28 (28d) days after the initial BrdU injection (l) as well as TUNEL (m), NeuroD (n) and Doublecortin (o) positive cells at 2 (2m-Dox) and 4 (4m-Dox) months after doxycycline removal. Infra, infrapyramidal blade; Supra, suprapyramidal blade; *t*-test, numbers indicate *P*-values; error bars, SEM; $n=3$ [4m-Dox in i,j,l,n (4d)]; $n=4$ [4m-Dox in l (28d), m; 2m-Dox in n; mutant in o]; $n=5$ (2m-Dox in i,j); $n=8$ (2m-Dox in l; control in o).

a significant reduction of apical thorny excrescences, the postsynaptic targets of mossy fiber terminals, was detected in mutants by Golgi impregnation (2m-Dox: control = 13.9 ± 1.35, mutant = 7 ± 0.78, $P=0.006$; 4m-Dox: control = 13.03 ± 0.34, mutant = 8.43 ± 0.49, $P=0.001$; Fig. 6c). Basal thorny excrescences were unchanged in mutants at 4 months after doxycycline removal (control = 18.37 ± 1.2, mutant = 19.5 ± 1.1; $P=0.265$) suggesting that the reduction in apical thorny excrescences is not because of a redistribution to the basal dendrites as was shown for hyperthyroid rats (Lauder & Mugnaini 1980). Furthermore, examining dendritic processes of granule cells did not show a reduction in the number of dendritic spines (control = 73.73 ± 2.1, mutant = 71.71 ± 2.4; $P=0.226$).

Adult-induced ablation of Bcl11b impairs learning and memory capacities

To determine learning and memory capacities of adult-induced *Bcl11b* mutants, animals were exposed to the open field test. At 2 months after doxycycline removal, we did not observe any significant changes in the behavior of control and *Bcl11b* mutants in all the tests performed (Fig. 7a–g,i,j).

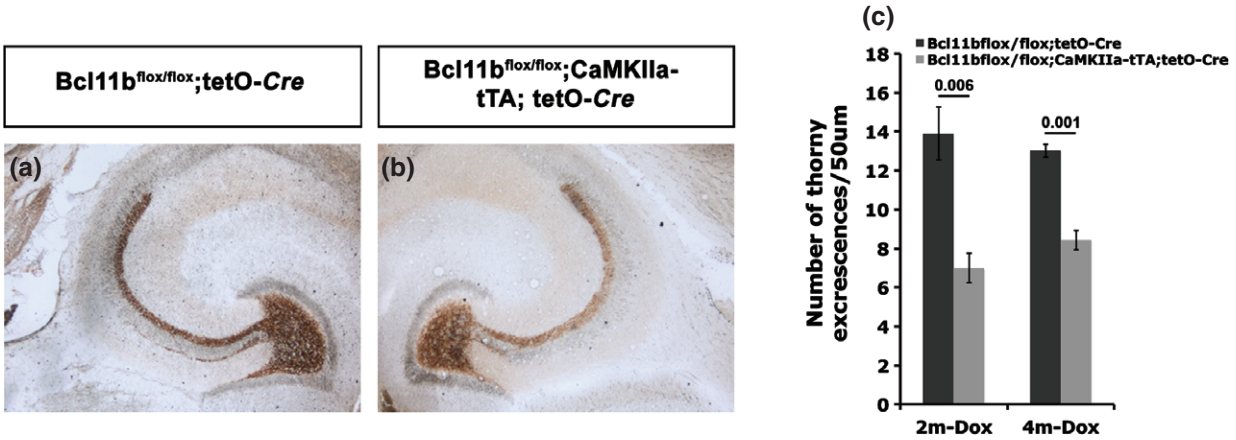

Figure 6: Analysis of hippocampal mossy fiber terminals of adult-induced *Bcl11b* mutants. (a,b) Timm staining of mossy fibers of control (a) and adult-induced *Bcl11b* mutant (b) hippocampi. (c) Quantitative analysis of apical thorny excrescences by Golgi impregnation of control and adult-induced *Bcl11b* mutant hippocampal sections at 2 (2m-Dox) and 4 (4m-Dox) months after doxycycline removal. *t*-test, numbers indicate *P*-values; error bars, SEM; $n = 3$.

In contrast, at 4 months after doxycycline removal we found behavioral deficiencies. Vertical activities (leaning and rearing) were significantly reduced in the *Bcl11b* mutant (leaning: control = 67.9 ± 9.1, mutant = 44.1 ± 7.1, $P = 0.042$; Fig. 7b; rearing: control = 49.7 ± 8.9, mutant = 22.1 ± 5.1, $P = 0.01$; Fig. 7c) while horizontal activities were unchanged (Fig. 7a,d) These data provided a first indication that ablation of *Bcl11b* expression in adulthood leads to spatial learning deficits. In addition, the eight-arm radial maze showed significant spatial learning deficits of the *Bcl11b* mutant. During the last 3 days of training, the *Bcl11b* mutants showed significantly fewer new entries within the first eight entries when compared with control animals (control = 6 ± 0.2, mutant = 5.4 ± 0.2; $P = 0.032$; Fig. 7e) and a significantly higher mean number of errors (control = 6.24 ± 0.55, mutant = 9.14 ± 0.9; $P = 0.009$; Fig. 7f). During the whole training period, the control mice made fewer errors, although only a trend toward better learning was found ($P = 0.07$; Fig. 7h). *Bcl11b* is also expressed in the amygdala (Leid *et al.* 2004), a brain region involved in anxiety-related processing. Analyzing the number of entries of closed vs. open arms did not show a significant difference between control and mutant animals (4m-Dox: control = 100 ± 0, mutant = 97.67 ± 2.3, $P = 0.169$; Fig. 7i), suggesting that the behavioral phenotype is not because of fear or anxiety behavior. However, we did observe a decrease of the total number of arms entered by the adult-induced mutant (4m-Dox: control = 27.43 ± 3.3, mutant = 19.14 ± 1.2, $P = 0.008$; Fig. 7j) showing an overall reduced activity of the adult mutant mice. Taken together, these data show that Bcl11b is required to establish and sustain a functional hippocampus. Ablation of Bcl11b selectively in adulthood results in an early morphological and late functional phenotype.

Discussion

In this study, we determined functions of the transcription factor Bcl11b specifically in the adult dentate gyrus of mice. Loss of *Bcl11b* expression selectively during adulthood results in an altered morphology with a reduced dentate gyrus size and granule cell number. Furthermore, we show Bcl11b to be required for the differentiation and structural integration of dentate granule neurons. Adult-born *Bcl11b* mutant dentate granule cells are arrested at the transition level from late progenitor stages to early immature postmitotic neurons and are unable to form correct contacts with their natural target neurons in CA3. Finally, we found that adult deletion of Bcl11b leads to impaired spatial learning capacities. Thus, our data show for the first time that Bcl11b is specifically required for sustaining structural and functional integrity of the adult hippocampus (data summarized in Table 2).

Bcl11b is required for the differentiation and survival of dentate granule cells

Adult neurogenesis of granule cells involves several factors expressed in a spatio-temporal pattern (reviewed in Hsieh 2012). It was shown previously that Bcl11b is required for cell type-specific differentiation in several brain regions (Arlotta *et al.* 2005, 2008; Simon *et al.* 2012) as well as in the hematopoietic system (Kastner *et al.* 2010; Liu *et al.* 2010; Wakabayashi *et al.* 2003). Analysis of the differentiation capacity of adult-born neurons showed that early stages of adult neurogenesis are not affected by the loss of *Bcl11b* expression. However, we found an arrest of adult-born neurons at the transition from the mitotic to postmitotic stage as indicated by an increase in NeuroD- and Doublecortin-positive cells in both mouse models. Similar observations were reported for the activity of the transcription factor PC3/Tis21 in dentate granule cells. Loss of PC3/Tis21 prevents terminal differentiation of adult-born granule cells resulting in the accumulation of immature neurons (Farioli-Vecchioli *et al.* 2009). In contrast, a decrease in NeuroD- and Doublecortin-positive cells was reported by the loss of transcription factors Prox1, a prospero-related homeobox gene, (Lavado *et al.* 2010) and

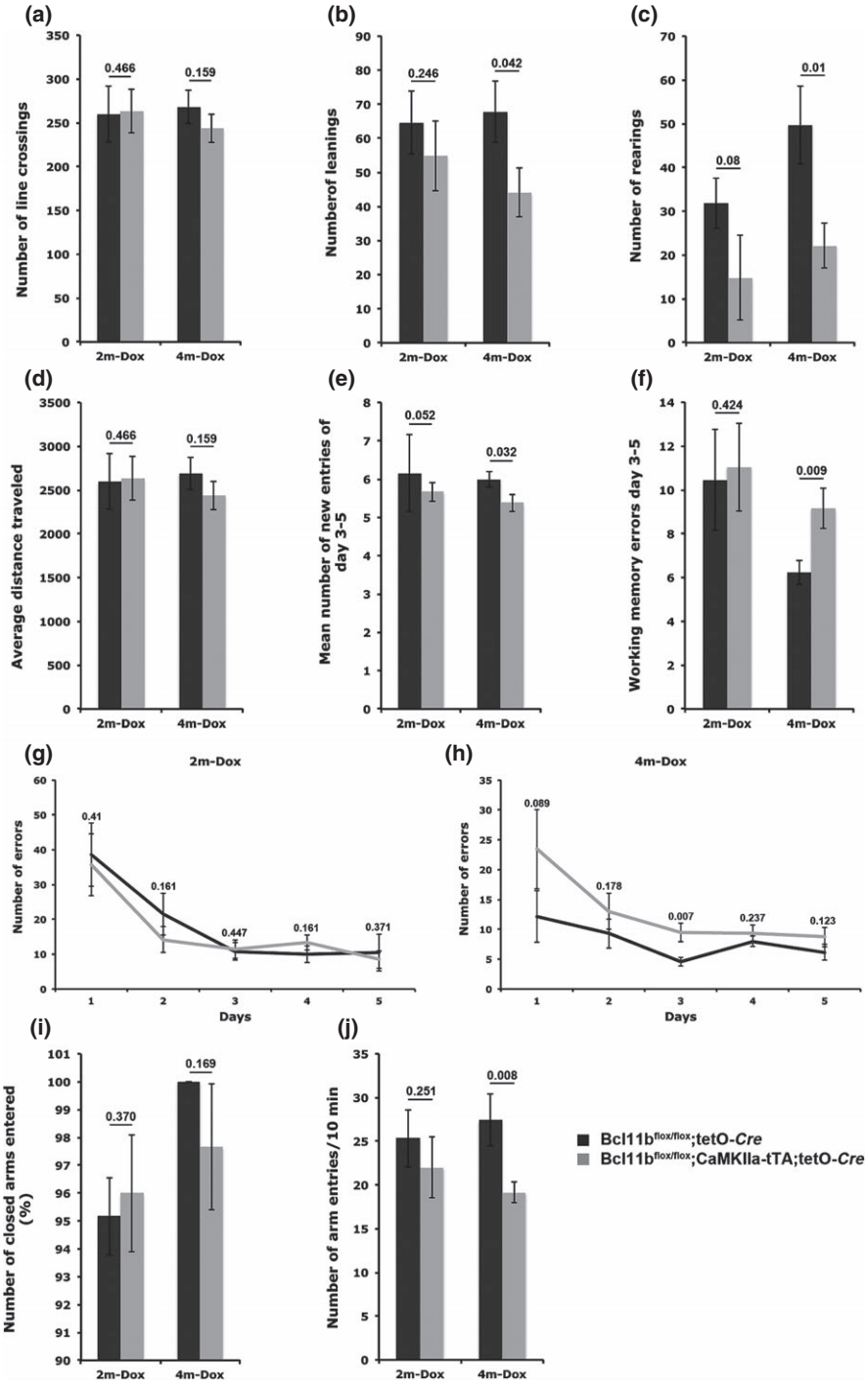

Figure 7: Adult-induced ablation of Bcl11b impairs spatial learning and working memory capacities at 4 months after doxycycline removal. (a–d) Open field test to determine locomotor activity (a), leaning (b) and rearing (c) events as well as distance traveled (d). (e–h) Radial maze test analysis of spatial learning behavior by determining new entries into radial arms (e) and working memory (f) at day 3–5 as well as number of errors at five successive days at 2 (2m-Dox) (g) and 4 (4m-Dox) (h) months after doxycycline removal. (i,j) Elevated plus maze test analyzing anxiety behavior. *t*-test, numbers indicate *P*-values; error bars, SEM; $n=6$ (2m-Dox); $n=7$ (4m-Dox).

cAMP response element-binding protein (CREB) (Jagasia *et al.* 2009). Both transcription factors are required for survival and maturation of newborn neurons during development and adulthood. *Prox1* is expressed in type 3 progenitor cells as well as in immature and mature neurons regulating also in a feedback mechanism the self-maintenance of neural stem cells (Lavado *et al.* 2010). On the other hand, CREB is required for the development of dendritic length and branching and integration of the mature neuron (Jagasia *et al.* 2009).

Examining conditional *Bcl11b* mutants showed a reduced progenitor cell proliferation rate during adult neurogenesis. In contrast, we did not observe a significant change in the progenitor cell proliferation rate of the adult-induced *Bcl11b* mutant. The difference in progenitor cell proliferation is

Table 2: Summary of the conditional and adult-induced Bcl11b phenotype. Analysis of the dentate gyrus area and cell number, progenitor cell proliferation, granule cell apoptosis, neuronal differentiation and number of thorny excrescences as well as spatial learning of *Bcl11b* conditional mutants at the age of 6 months and adult-induced *Bcl11b* mutants 2 (2m-Dox) and 4 months (4m-Dox) after doxycycline removal.

	Conditional mutant	Adult-induced mutant	
Age	6 months	4 months 2m-Dox	6 months 4m-Dox
Dentate gyrus area	↓	↓	n.c.
Number of granule cells	↓	↓	n.c.
Proliferation of progenitor cells	↓	n.c.	n.c.
Apoptosis	n.c.	↑	↑
Differentiation of postmitotic neurons	↓	↓	↓
Thorny excrescences	↓*	↓	↓
Spatial learning	↓*	n.c.	↓

Arrows indicate increase or decrease of parameters determined. n.c., not changed.
*Simon *et al.* 2012.

unlikely because of the different *Cre*-mouse lines used. While Emx1 is expressed in mitotic and postmitotic cells, *CaMKIIα*, like *Bcl11b*, is expressed only in postmitotic cells. Therefore, Bcl11b regulation of progenitor cell proliferation occurs in a non-cell autonomous signaling pathway. Furthermore, a comparison of the phenotypes of *Bcl11b*$^{flox/flox}$; *Emx1-Cre* and *Bcl11b*$^{flox/flox}$; *Nex-Cre* mutant, a *Cre*-mouse line active only in postmitotic neurons, did not show any differences (Simon *et al.* 2012). The difference in progenitor cell proliferation of the two mouse models used in this study is more likely because of the size of the progenitor cell pool. In the conditional mutant, the number of progenitor cells is reduced during postnatal development with fewer cells present to undergo adult neurogenesis. In the adult-induced mouse model, the progenitor cell pool is not affected during development and should be indistinguishable in control and mutant. The significant reduction of BrdU-positive cells at a late time point (28 days; 4m-Dox; Fig. 5l) is most likely because of the reduced survival rate of mutant granule cells.

Analyzing adult-induced *Bcl11b* mutant mice showed a surprising reduction of size and cell number of a normally developed dentate gyrus most likely caused by the dramatic increase of apoptotic cells, strongly suggesting that Bcl11b is required for the survival of mature granule cells. This is supported by our data showing an unchanged progenitor cell proliferation rate. Furthermore, it was previously reported that an arrest of adult neurogenesis does not cause any changes in the size of the dentate gyrus (Raber *et al.* 2004).

Transcription factors are not only required for the initiation of the terminal differentiation but are also essential to maintain the specificity of differentiated cells (reviewed in Deneris & Hobert 2014). Such a function was suggested for chicken ovalbumin upstream promoter transcription factor (COUP-TF) in the maintenance of dopaminergic interneurons of the olfactory bulbs by regulating tyrosine hydroxylase expression (Bovetti *et al.* 2013). Previously, it was shown that COUP-TFI and Bcl11b are interacting in the regulation of the expression of target genes (Avram *et al.* 2000). Although no such interaction of Bcl11b and COUP-TFI was reported yet in the dentate gyrus, it is possible that Bcl11b by itself regulates the expression of its target genes affecting the maintenance of granule cells as was shown for the closely related transcription factors Bcl11a and Bcl-2, a factor involved in the regulation of apoptosis (Yu *et al.* 2012).

Ablation of Bcl11b leads to the downregulation of *Dsp*, a cell adhesion molecule, in the dentate gyrus (Fig. 4b; Simon *et al.* 2012). By examining the conditional *Dsp* mutant during postnatal dentate gyrus development, we observed a downregulation of apoptosis as well as progenitor cell proliferation and neuronal differentiation (Simon *et al.* 2012). However, it is conceivable that Dsp executes different functions during hippocampal development vs. adulthood similar to Bcl11b. One could therefore argue that Bcl11b and in particular Dsp are required to stabilize granule cells and/or their cell–cell contacts. It is well known that Dsp interacts with intermediate filaments, microtubule-associated proteins as well as members of the catenin protein family such as Plakoglobin to stabilize the cytoskeleton (Garcia-Gras *et al.* 2006; Sumigray *et al.* 2011). In neurons, the cytoskeleton executes an important function in the axonal transport of mitochondria, vesicles and mRNA among others (reviewed in Chevalier-Larsen & Holzbaur 2006). Dysfunction of the axonal transport can lead to cell death and is associated with a number of neurodegenerative diseases such as amyotrophic lateral sclerosis and Alzheimer's disease (Alami *et al.* 2014; Manfredi & Xu 2005; reviewed in Zempel & Mandelkow 2014). It is feasible that Bcl11b regulates factors involved in the cytoskeleton and loss of Bcl11b in adulthood leads to the destabilization of the cytoskeleton causing impairment of axonal transport and cell death.

Furthermore, degeneration of mature and integrated dentate gyrus granule cells can also be caused by the ablation of factors like *N*-methyl-D-aspartate receptors (NMDA receptors) and nuclear factor kappaB (NF-κB) leading to impairment of memory capacities (Imielski *et al.* 2012; Watanabe *et al.* 2016). Interestingly, both factors, like Bcl11b, have distinct functions in immature and mature neurons. This is the case in particular for NF-κB which regulates axon formation and maturation in progenitor cells as well as survival and synaptic activity in mature neurons (Imielski *et al.* 2012). In addition, the authors showed that re-activation of NF-κB rescued the phenotype in the adult brain suggesting NF-κB as a

therapeutic target (Imielski *et al.* 2012). Intriguingly, it was shown previously that Bcl11b is involved in the regulation of NF-κB in T-lymphocytes by activating Cot (Cancer Osaka thyroid oncogene) kinase expression (Cismasiu *et al.* 2009). In our report, we are providing further evidence of adult-specific functions of Bcl11b. Taken together, this raises the question whether Bcl11b might be involved in a similar regulatory mechanism of NF-κB in the brain and loss of *Bcl11b* expression leading to cell death of mature and integrated granule cells via reduced NF-κB activity.

Ablation of Bcl11b in adulthood causes impairment of spatial learning and memory

It is well established that changes in the hippocampal morphology result in modified functions such as spatial learning and memory (Crusio & Schwegler 2005; Crusio *et al.* 1989) and neurodegenerative diseases like schizophrenia and Alzheimer's (Kolomeets *et al.* 2007; Yeung *et al.* 2014). Depending on the lesion of the dentate gyrus, different hippocampal functions are affected. Lesions of the dorsal hippocampus impair spatial learning, whereas lesions of the ventral part change anxiety behavior (Bannerman *et al.* 2004). Although we see a dramatic loss of granule cells and reduction of the dentate gyrus area already at 2 months after doxycycline removal, the behavioral impairment was only evident at 4 months after the induction of the *Bcl11b* mutation. At this time, the adult-induced *Bcl11b* mutants displayed a deficit in spatial working memory. We also noticed that the *Bcl11b*$^{flox/flox}$; *tetO-Cre* control animals exhibited a reduced learning and memory capacity when compared with the conditional *Bcl11b*$^{flox/+}$; *Emx1-Cre* control animals. This might be because of 'leakiness' of the *Cre*-system (Delerue *et al.* 2014) causing a partial premature induction of the mutation in both control and mutant animals. To compensate for this leakiness, we used *Bcl11b*$^{flox/flox}$; *tetO-Cre* (control) and *Bcl11b*$^{flox/flox}$; *CaMKII*α*-tTA*; *tetO-Cre* (mutant) animals for our experiments. Comparing the conditional and adult-induced *Bcl11b* mutants showed a weaker behavioral phenotype with the inducible system (Simon *et al.* 2012), which could be because of the effect of Bcl11b ablation during hippocampal development.

In the adult-induced *Bcl11b* mutant, we observed a less severe mossy fiber tract phenotype. Once established the main trajectories of the mossy fibers remain stable throughout life (H. Schwegler, unpublished observations), which might explain the overall unchanged distribution pattern in the adult-induced *Bcl11b* mutant in comparison to the aberrant projection pattern of mossy fibers in the conditional mouse model (Simon *et al.* 2012). In contrast, thorny excrescences, located in the suprapyramidal mossy fiber tract and responsible for consolidating working memory (Gaarskjaer 1986), are more sensitive to changes. A reduction of mossy fiber synapses can be linked to diseases as was shown for schizophrenia (Kolomeets *et al.* 2007). In both *Bcl11b* mouse models, the number of apical thorny excrescences is significantly reduced but no redistribution to the basal dendrites was observed. Although there are fewer mossy fibers because of the reduced number of granule cells, we did not observe a change in the overall pattern of the mossy fiber tract, but the reduced number of granule cells might lead to fewer thorny excrescences. The reduction of mossy fibers and thorny excrescences can be compensated by mossy fiber sprouting of the remaining established mossy fibers restoring synaptic plasticity at least to some degree which was shown in particular for overtraining of spatial tasks (Ramirez-Amaya *et al.* 1999) and epileptic episodes (Lin *et al.* 2011). Similarly, mossy fiber sprouting could be the first reaction to the sudden loss of granule cells caused by the ablation of Bcl11b rescuing the synaptic plasticity and therefore delaying the behavioral phenotype.

The adult-induced Bcl11b mutation causes an immediate morphological and late functional phenotype

Lack of *Bcl11b* expression during development prevents to develop a functional hippocampus deteriorating further throughout life. Inducing the *Bcl11b* mutation only in adulthood, in the presence of an established hippocampal circuitry, causes immediate dramatic morphological changes but surprisingly a delayed functional impairment (Table 2). The dentate gyrus area and cell number are dramatically decreased already at 2 months after doxycycline removal with no further reduction in the following 2 months. Surprisingly, functional changes such as spatial learning and memory behavior were only observed at a later time point in the adult-induced *Bcl11b* mutant and are less severe when compared with the conditional *Bcl11b* mutant (Simon *et al.* 2012). An explanation could be that once established hippocampal structures are more robust to morphological changes and are able to compensate for the loss of granule cells up to a certain degree before learning and memory capacities are affected as was shown for mossy fibers (Lin *et al.* 2011). Taken together, Bcl11b executes crucial functions in both postnatal as well as adult neurogenesis by establishing a functional dentate gyrus during postnatal development and most importantly maintaining the neuronal circuitry during adulthood.

In context to human pathology, there is no direct evidence up to date for the involvement of Bcl11b in neurodegenerative diseases. Recently, it was reported that Bcl11a, a closely related transcription factor of Bcl11b, might be a candidate gene of disorders such as autism, apraxia of speech and microcephaly among others (Basak *et al.* 2015; Hancarova *et al.* 2013; Peter *et al* 2014). It is possible that Bcl11b executes functions in human hippocampal development and adult neurogenesis comparable to our mouse models. Thus, a loss of *Bcl11b* expression in human hippocampal neurogenesis could contribute to neurodevelopmental defects as well as diseases in adulthood such dementia, Alzheimer's and schizophrenia.

References

Alami, N.H., Smith, R.B., Carrasco, M.A., Williams, L.A., Winborn, C.S., Han, S.S., Kiskinis, E., Winborn, B., Freibaum, B.D., Kanagaraj, A., Clare, A.J., Badders, N.M., Bilican, B., Chaum, E., Chandran, S., Shaw, C.E., Eggan, K.C., Maniatis, T. & Taylor, J.P. (2014) Axonal transport of TDP-43 mRNA granules is impaired by ALS-causing mutations. *Neuron* **81**, 536–543.

Altman, J. & Bayer, S.A. (1990) Migration and distribution of two populations of hippocampal granule cell precursors during the perinatal and postnatal periods. *J Comp Neurol* **301**, 365–381.

Arlotta, P., Molyneaux, B.J., Chen, J., Inoue, J., Kominami, R. & Macklis, J.D. (2005) Neuronal subtype-specific genes that control corticospinal motor neuron development in vivo. *Neuron* **45**, 207–221.

Arlotta, P., Molyneaux, B.J., Jabaudon, D., Yoshida, Y. & Macklis, J.D. (2008) Ctip2 controls the differentiation of medium spiny neurons and the establishment of the cellular architecture of the striatum. *J Neurosci* **28**, 622–632.

Avram, D., Fields, A., Pretty on Top, K., Nevrivy, D.J., Ishmael, J.E. & Leid, M. (2000) Isolation of a novel family of C(2)H(2) zinc finger proteins implicated in transcriptional repression mediated by chicken ovalbumin upstream promoter transcription factor (COUP-TF) orphan nuclear receptors. *J Biol Chem* **275**, 10315–10322.

Bannerman, D.M., Rawlins, J.N., Mchugh, S.B., Deacon, R.M., Yee, B.K., Bast, T., Zhang, W.N., Pothuizen, H.H. & Feldon, J. (2004) Regional dissociations within the hippocampus–memory and anxiety. *Neurosci Biobehav Rev* **28**, 273–283.

Basak, A., Hancarova, M., Ulirsch, J.C., Balci, T.B., Trkova, M., Pelisek, M., Vlckova, M., Muzikova, K., Cermak, J., Trka, J., Dyment, D.A., Orkin, S.H., Daly, M.J., Sedlacek, Z. & Sankaran, V.G. (2015) BCL11A deletions result in fetal hemoglobin persistence and neurodevelopmental alterations. *J Clin Invest* **125**, 2363–2368.

Bovetti, S., Bonzano, S., Garzotto, D., Giannelli, S.G., Iannielli, A., Armentano, M., Studer, M. & De Marchis, S. (2013) COUP-TFI controls activity-dependent tyrosine hydroxylase expression in adult dopaminergic olfactory bulb interneurons. *Development* **140**, 4850–4859.

Burgin, K.E., Waxham, M.N., Rickling, S., Westgate, S.A., Mobley, W.C. & Kelly, P.T. (1990) In situ hybridization histochemistry of Ca2+/calmodulin-dependent protein kinase in developing rat brain. *J Neurosci* **10**, 1788–1798.

Chen, B., Wang, S.S., Hattox, A.M., Rayburn, H., Nelson, S.B. & Mcconnell, S.K. (2008) The Fezf2-Ctip2 genetic pathway regulates the fate choice of subcortical projection neurons in the developing cerebral cortex. *Proc Natl Acad Sci U S A* **105**, 11382–11387.

Chevalier-Larsen, E. & Holzbaur, E.L. (2006) Axonal transport and neurodegenerative disease. *Biochim Biophys Acta* **1762**, 1094–1108.

Cismasiu, V.B., Ghanta, S., Duque, J., Albu, D.I., Chen, H.M., Kasturi, R. & Avram, D. (2006) BCL11B participates in the activation of IL2 gene expression in CD4+ T lymphocytes. *Blood* **108**, 2695–2702.

Cismasiu, V.B., Duque, J., Paskaleva, E., Califano, D., Ghanta, S., Young, H.A. & Avram, D. (2009) BCL11B enhances TCR/CD28-triggered NF-kappaB activation through up-regulation of Cot kinase gene expression in T-lymphocytes. *Biochem J* **417**, 457–466.

Crusio, W.E. & Schwegler, H. (2005) Learning spatial orientation tasks in the radial-maze and structural variation in the hippocampus in inbred mice. *Behav Brain Funct* **1**, 3.

Crusio, W.E., Schwegler, H., Brust, I. & Van Abeelen, J.H. (1989) Genetic selection for novelty-induced rearing behavior in mice produces changes in hippocampal mossy fiber distributions. *J Neurogenet* **5**, 87–93.

Delerue, F., White, M. & Ittner, L.M. (2014) Inducible, tightly regulated and non-leaky neuronal gene expression in mice. *Transgenic Res* **23**, 225–233.

Deneris, E.S. & Hobert, O. (2014) Maintenance of postmitotic neuronal cell identity. *Nat Neurosci* **17**, 899–907.

Deng, W., Aimone, J.B. & Gage, F.H. (2010) New neurons and new memories: how does adult hippocampal neurogenesis affect learning and memory? *Nat Rev Neurosci* **11**, 339–350.

Ehret, F., Vogler, S., Pojar, S., Elliott, D.A., Bradke, F., Steiner, B. & Kempermann, G. (2015) Mouse model of CADASIL reveals novel insights into Notch3 function in adult hippocampal neurogenesis. *Neurobiol Dis* **75**, 131–141.

Farioli-Vecchioli, S., Saraulli, D., Costanzi, M., Leonardi, L., Cina, I., Micheli, L., Nutini, M., Longone, P., Oh, S.P., Cestari, V. & Tirone, F. (2009) Impaired terminal differentiation of hippocampal granule neurons and defective contextual memory in PC3/Tis21 knockout mice. *PLoS One* **4**, e8339.

Farioli-Vecchioli, S., Mattera, A., Micheli, L., Ceccarelli, M., Leonardi, L., Saraulli, D., Costanzi, M., Cestari, V., Rouault, J.P. & Tirone, F. (2014) Running rescues defective adult neurogenesis by shortening the length of the cell cycle of neural stem and progenitor cells. *Stem Cells* **32**, 1968–1982.

Gaarskjaer, F.B. (1986) The organization and development of the hippocampal mossy fiber system. *Brain Res* **396**, 335–357.

Garcia-Gras, E., Lombardi, R., Giocondo, M.J., Willerson, J.T., Schneider, M.D., Khoury, D.S. & Marian, A.J. (2006) Suppression of canonical Wnt/beta-catenin signaling by nuclear plakoglobin recapitulates phenotype of arrhythmogenic right ventricular cardiomyopathy. *J Clin Invest* **116**, 2012–2021.

Gibbons, T.E., Pence, B.D., Petr, G., Ossyra, J.M., Mach, H.C., Bhattacharya, T.K., Perez, S., Martin, S.A., Mccusker, R.H., Kelley, K.W., Rhodes, J.S., Johnson, R.W. & Woods, J.A. (2014) Voluntary wheel running, but not a diet containing (-)-epigallocatechin-3-gallate and beta-alanine, improves learning, memory and hippocampal neurogenesis in aged mice. *Behav Brain Res* **272**, 131–140.

Gonzales, R.B., Deleon Galvan, C.J., Rangel, Y.M. & Claiborne, B.J. (2001) Distribution of thorny excrescences on CA3 pyramidal neurons in the rat hippocampus. *J Comp Neurol* **430**, 357–368.

Gorski, J.A., Talley, T., Qiu, M., Puelles, L., Rubenstein, J.L. & Jones, K.R. (2002) Cortical excitatory neurons and glia, but not GABAergic neurons, are produced in the Emx1-expressing lineage. *J Neurosci* **22**, 6309–6314.

Hancarova, M., Simandlova, M., Drabova, J., Mannik, K., Kurg, A. & Sedlacek, Z. (2013) A patient with de novo 0.45 Mb deletion of 2p16.1: the role of BCL11A, PAPOLG, REL, and FLJ16341 in the 2p15-p16.1 microdeletion syndrome. *Am J Med Genet A* **161A**, 865–870.

Heimrich, B. & Frotscher, M. (1991) Differentiation of dentate granule cells in slice cultures of rat hippocampus: a Golgi/electron microscopic study. *Brain Res* **538**, 263–268.

Heinrich, C., Nitta, N., Flubacher, A., Muller, M., Fahrner, A., Kirsch, M., Freiman, T., Suzuki, F., Depaulis, A., Frotscher, M. & Haas, C.A. (2006) Reelin deficiency and displacement of mature neurons, but not neurogenesis, underlie the formation of granule cell dispersion in the epileptic hippocampus. *J Neurosci* **26**, 4701–4713.

Hsieh, J. (2012) Orchestrating transcriptional control of adult neurogenesis. *Genes Dev* **26**, 1010–1021.

Imielski, Y., Schwamborn, J.C., Luningschror, P., Heimann, P., Holzberg, M., Werner, H., Leske, O., Puschel, A.W., Memet, S., Heumann, R., Israel, A., Kaltschmidt, C. & Kaltschmidt, B. (2012) Regrowing the adult brain: NF-kappaB controls functional circuit formation and tissue homeostasis in the dentate gyrus. *PLoS One* **7**, e30838.

Jagasia, R., Steib, K., Englberger, E., Herold, S., Faus-Kessler, T., Saxe, M., Gage, F.H., Song, H. & Lie, D.C. (2009) GABA-cAMP response element-binding protein signaling regulates maturation and survival of newly generated neurons in the adult hippocampus. *J Neurosci* **29**, 7966–7977.

Jiang, Y. & Hsieh, J. (2014) HDAC3 controls gap 2/mitosis progression in adult neural stem/progenitor cells by regulating CDK1 levels. *Proc Natl Acad Sci U S A* **111**, 13541–13546.

Kastner, P., Chan, S., Vogel, W.K., Zhang, L.J., Topark-Ngarm, A., Golonzhka, O., Jost, B., Le Gras, S., Gross, M.K. & Leid, M. (2010) Bcl11b represses a mature T-cell gene expression program in immature CD4(+)CD8(+) thymocytes. *Eur J Immunol* **40**, 2143–2154.

Kempermann, G. (2011) *Adult Neurogenesis 2: Stem Cells and Neuronal Development in the Adult Brain*. Oxford University Press, Oxford, UK.

Kempermann, G., Gast, D., Kronenberg, G., Yamaguchi, M. & Gage, F.H. (2003) Early determination and long-term persistence of adult-generated new neurons in the hippocampus of mice. *Development* **130**, 391–399.

Kempermann, G., Wiskott, L. & Gage, F.H. (2004) Functional significance of adult neurogenesis. *Curr Opin Neurobiol* **14**, 186–191.

Klempin, F. & Kempermann, G. (2007) Adult hippocampal neurogenesis and aging. *Eur Arch Psychiatry Clin Neurosci* **257**, 271–280.

Kolomeets, N.S., Orlovskaya, D.D. & Uranova, N.A. (2007) Decreased numerical density of CA3 hippocampal mossy fiber synapses in schizophrenia. *Synapse* **61**, 615–621.
Lauder, J.M. & Mugnaini, E. (1980) Infrapyramidal mossy fibers in the hippocampus of the hyperthyroid rat. A light and electron microscopic study. *Dev Neurosci* **3**, 248–265.
Lavado, A., Lagutin, O.V., Chow, L.M., Baker, S.J. & Oliver, G. (2010) Prox1 is required for granule cell maturation and intermediate progenitor maintenance during brain neurogenesis. *PLoS Biol* **8**(8): e1000460. doi:10.1371/journal.pbio.1000460.
Leid, M., Ishmael, J.E., Avram, D., Shepherd, D., Fraulob, V. & Dolle, P. (2004) CTIP1 and CTIP2 are differentially expressed during mouse embryogenesis. *Gene Expr Patterns* **4**, 733–739.
Li, G. & Pleasure, S.J. (2005) Morphogenesis of the dentate gyrus: what we are learning from mouse mutants. *Dev Neurosci* **27**, 93–99.
Li, G. & Pleasure, S.J. (2007) Genetic regulation of dentate gyrus morphogenesis. *Prog Brain Res* **163**, 143–152.
Li, P., Burke, S., Wang, J., Chen, X., Ortiz, M., Lee, S.C., Lu, D., Campos, L., Goulding, D., Ng, B.L., Dougan, G., Huntly, B., Gottgens, B., Jenkins, N.A., Copeland, N.G., Colucci, F. & Liu, P. (2010) Reprogramming of T cells to natural killer-like cells upon Bcl11b deletion. *Science* **329**, 85–89.
Lie, D.C., Colamarino, S.A., Song, H.J., Desire, L., Mira, H., Consiglio, A., Lein, E.S., Jessberger, S., Lansford, H., Dearie, A.R. & Gage, F.H. (2005) Wnt signalling regulates adult hippocampal neurogenesis. *Nature* **437**, 1370–1375.
Lin, H., Huang, Y., Wang, Y. & Jia, J. (2011) Spatiotemporal profile of N-cadherin expression in the mossy fiber sprouting and synaptic plasticity following seizures. *Mol Cell Biochem* **358**, 201–205.
Liu, P., Li, P. & Burke, S. (2010) Critical roles of Bcl11b in T-cell development and maintenance of T-cell identity. *Immunol Rev* **238**, 138–149.
Livak, K.J. & Schmittgen, T.D. (2001) Analysis of relative gene expression data using real-time quantitative PCR and the 2(-Delta Delta C(T)) Method. *Methods* **25**, 402–408.
Manfredi, G. & Xu, Z. (2005) Mitochondrial dysfunction and its role in motor neuron degeneration in ALS. *Mitochondrion* **5**, 77–87.
Mathews, E.A., Morgenstern, N.A., Piatti, V.C., Zhao, C., Jessberger, S., Schinder, A.F. & Gage, F.H. (2010) A distinctive layering pattern of mouse dentate granule cells is generated by developmental and adult neurogenesis. *J Comp Neurol* **518**, 4479–4490.
Mayford, M., Bach, M.E., Huang, Y.Y., Wang, L., Hawkins, R.D. & Kandel, E.R. (1996) Control of memory formation through regulated expression of a CaMKII transgene. *Science* **274**, 1678–1683.
Mirescu, C. & Gould, E. (2006) Stress and adult neurogenesis. *Hippocampus* **16**, 233–238.
Muramatsu, R., Ikegaya, Y., Matsuki, N. & Koyama, R. (2007) Neonatally born granule cells numerically dominate adult mice dentate gyrus. *Neuroscience* **148**, 593–598.
Pereira, J.B., Junque, C., Bartres-Faz, D., Ramirez-Ruiz, B., Marti, M.J. & Tolosa, E. (2013) Regional vulnerability of hippocampal subfields and memory deficits in Parkinson's disease. *Hippocampus* **23**, 720–728.
Peter, B., Matsushita, M., Oda, K. & Raskind, W. (2014) De novo microdeletion of BCL11A is associated with severe speech sound disorder. *Am J Med Genet A* **164A**, 2091–2096.
Raber, J., Fan, Y., Matsumori, Y., Liu, Z., Weinstein, P.R., Fike, J.R. & Liu, J. (2004) Irradiation attenuates neurogenesis and exacerbates ischemia-induced deficits. *Ann Neurol* **55**, 381–389.
Ramirez-Amaya, V., Escobar, M.L., Chao, V. & Bermudez-Rattoni, F. (1999) Synaptogenesis of mossy fibers induced by spatial water maze overtraining. *Hippocampus* **9**, 631–636.
Sahay, A. & Hen, R. (2007) Adult hippocampal neurogenesis in depression. *Nat Neurosci* **10**, 1110–1115.
Schwegler, H. & Lipp, H.P. (1983) Hereditary covariations of neuronal circuitry and behavior: correlations between the proportions of hippocampal synaptic fields in the regio inferior and two-way avoidance in mice and rats. *Behav Brain Res* **7**, 1–38.
Schwegler, H., Crusio, W.E. & Brust, I. (1990) Hippocampal mossy fibers and radial-maze learning in the mouse: a correlation with spatial working memory but not with non-spatial reference memory. *Neuroscience* **34**, 293–298.
Simon, R., Brylka, H., Schwegler, H., Venkataramanappa, S., Andratschke, J., Wiegreffe, C., Liu, P., Fuchs, E., Jenkins, N.A., Copeland, N.G., Birchmeier, C. & Britsch, S. (2012) A dual function of Bcl11b/Ctip2 in hippocampal neurogenesis. *EMBO J* **31**, 2922–2936.
Sirerol-Piquer, M., Gomez-Ramos, P., Hernandez, F., Perez, M., Moran, M.A., Fuster-Matanzo, A., Lucas, J.J., Avila, J. & Garcia-Verdugo, J.M. (2011) GSK3beta overexpression induces neuronal death and a depletion of the neurogenic niches in the dentate gyrus. *Hippocampus* **21**, 910–922.
Sumigray, K.D., Chen, H. & Lechler, T. (2011) Lis1 is essential for cortical microtubule organization and desmosome stability in the epidermis. *J Cell Biol* **194**, 631–642.
Topark-Ngarm, A., Golonzhka, O., Peterson, V.J., Barrett, B. Jr., Martinez, B., Crofoot, K., Filtz, T.M. & Leid, M. (2006) CTIP2 associates with the NuRD complex on the promoter of p57KIP2, a newly identified CTIP2 target gene. *J Biol Chem* **281**, 32272–32283.
Urban, N. & Guillemot, F. (2014) Neurogenesis in the embryonic and adult brain: same regulators, different roles. *Front Cell Neurosci* **8**, 396.
Van Praag, H., Christie, B.R., Sejnowski, T.J. & Gage, F.H. (1999) Running enhances neurogenesis, learning, and long-term potentiation in mice. *Proc Natl Acad Sci U S A* **96**, 13427–13431.
Wakabayashi, Y., Watanabe, H., Inoue, J., Takeda, N., Sakata, J., Mishima, Y., Hitomi, J., Yamamoto, T., Utsuyama, M., Niwa, O., Aizawa, S. & Kominami, R. (2003) Bcl11b is required for differentiation and survival of alphabeta T lymphocytes. *Nat Immunol* **4**, 533–539.
Watanabe, Y., Muller, M.K., Von Engelhardt, J., Sprengel, R., Seeburg, P.H. & Monyer, H. (2016) Age-dependent degeneration of mature dentate gyrus granule cells following NMDA receptor ablation. *Front Mol Neurosci* **8**, 87.
Winner, B. & Winkler, J. (2015) Adult neurogenesis in neurodegenerative diseases. *Cold Spring Harb Perspect Biol* **7**, a021287.
Yeung, S.T., Myczek, K., Kang, A.P., Chabrier, M.A., Baglietto-Vargas, D. & Laferla, F.M. (2014) Impact of hippocampal neuronal ablation on neurogenesis and cognition in the aged brain. *Neuroscience* **259**, 214–222.
Yilmazer-Hanke, D.M., Wigger, A., Linke, R., Landgraf, R. & Schwegler, H. (2004) Two Wistar rat lines selectively bred for anxiety-related behavior show opposite reactions in elevated plus maze and fear-sensitized acoustic startle tests. *Behav Genet* **34**, 309–318.
Yu, Y., Wang, J., Khaled, W., Burke, S., Li, P., Chen, X., Yang, W., Jenkins, N.A., Copeland, N.G., Zhang, S. & Liu, P. (2012) Bcl11a is essential for lymphoid development and negatively regulates p53. *J Exp Med* **209**, 2467–2483.
Zempel, H. & Mandelkow, E. (2014) Lost after translation: missorting of Tau protein and consequences for Alzheimer disease. *Trends Neurosci* **37**, 721–732.

Acknowledgments

This work was supported by grants from the Deutsche Forschungsgemeinschaft to S.B. (SFB 497/A9 and BR-2215) and fellowships by the International Graduate School in Molecular Medicine of the Ulm University to L.B. and E.D.B. This work was supported in part by the Cancer Research Institute of Texas (to N.G.C. and N.A.J.). N.G.C. and N.A.J. are also Cancer Prevention Research Institute of Texas Scholars in Cancer Research. We thank Jacqueline Andratschke, Sachi Takenaka and Elena Werle for excellent technical support.